

Nanoscale

Accepted Manuscript



This is an *Accepted Manuscript*, which has been through the Royal Society of Chemistry peer review process and has been accepted for publication.

Accepted Manuscripts are published online shortly after acceptance, before technical editing, formatting and proof reading. Using this free service, authors can make their results available to the community, in citable form, before we publish the edited article. We will replace this *Accepted Manuscript* with the edited and formatted *Advance Article* as soon as it is available.

You can find more information about *Accepted Manuscripts* in the [Information for Authors](#).

Please note that technical editing may introduce minor changes to the text and/or graphics, which may alter content. The journal's standard [Terms & Conditions](#) and the [Ethical guidelines](#) still apply. In no event shall the Royal Society of Chemistry be held responsible for any errors or omissions in this *Accepted Manuscript* or any consequences arising from the use of any information it contains.



Journal Name

ARTICLE

Inkjet printed fluorescent nanorods layers exhibit superior optical performance over quantum dots

Shira Halivni,^a Shay Shemesh,^a Nir Waiskopf,^a Yelena Vinetsky,^a Shlomo Magdassi,^a and Uri Banin^a

Received 00th January 20xx,
Accepted 00th January 20xx

DOI: 10.1039/x0xx00000x

www.rsc.org/

Semiconductor nanocrystals exhibit unique fluorescent properties which are tunable by size, shape and composition. Their high quantum yield and enhanced stability led to their use in biomedical imaging and flat panel displays. Here, semiconductor nanorods based inkjet inks are presented, overcoming limitations of the commonly reported quantum dots in printing applications. Fluorescent seeded nanorods were found as outstanding candidates for fluorescent inks, due to their low particle-particle interactions and negligible self-absorption. This is manifested by insignificant emission shifts upon printing, even at highly concentrated printed layers and by maintaining the high fluorescence quantum yield, unlike quantum dots which exhibit fluorescent wavelength shifts and quenching effects. This behavior results from the reduced absorption/emission overlap, accompanied by low energy transfer efficiencies between the nanorods as supported by steady state and time resolved fluorescence measurements. The new seeded nanorods inks enable patterning of uniform fluorescent layers, for demanding light emission applications such as signage and displays.

Introduction

In the last few years, fluorescent semiconductor nanocrystals (NCs) have developed greatly in terms of control of their size, shape and composition providing exceptional control over their properties allowing for their implementation in a variety of applications.¹⁻⁶ The NCs are characterized by a wide absorption spectrum accompanied by a narrow and sharp emission spectrum at the band edge, which enable the simultaneous excitation of NCs with different emission wavelengths using the same lighting source. The fluorescent semiconductor NCs also show outstanding optical and chemical stability under light irradiation over long periods of time.⁷ Their surface chemistry can also be adjusted for dispersion in a specific medium, both in organic and polar media, by proper selection of the stabilizing moieties.^{8, 9} The combination of these optical and chemical characteristics renders the NCs as excellent candidates for serving as building blocks in applications in a variety of fields. One approach used to achieve applicable devices is layer deposition by different printing techniques,¹⁰⁻¹⁴ in particular, semiconductor NCs have been recently introduced successfully into flat panel displays, serving as colour converters providing liquid crystal displays with exceptional high colour gamut and brightness.¹⁵⁻²¹ All this calls for further development and study into methods for

patterning fluorescent semiconductor nanocrystals in a robust and reproducible manner.

Inkjet printing is an important wet deposition method for nanoparticles,²² which is commonly used in industrial and domestic applications. Previous reports discuss the printing of nanoparticles; the inkjet printing of metallic nanoparticles for conductive electrodes is well established in the literature.²³⁻²⁸ Inkjet printing of fluorescent semiconductor NCs quantum dots (QDs) was also reported.²⁹⁻³⁸

Although there are many advantages for the use of fluorescent semiconductor NCs QDs for printing applications, their arrangement in proximity on a substrate leads to optical interference due to particle-particle interactions. These interactions may result in Forster type fluorescence resonance energy transfer (FRET) as well as in self-absorption effects. The phenomenon of self-absorption, in which particles absorb the light emitted by other particles, is highly pronounced in QDs, even after a growth of an outer shell on the core. This phenomenon is caused by the significant overlap between the absorption and the emission spectra of the QDs, which leads to efficient re-absorption of the emission. The self-absorption effect causes the effective external emission quantum yield (QY) to decrease significantly and induces changes in the fluorescent colour by shifting the emission energy to longer wavelengths. A similar degradation in emission properties is also induced by the FRET process by which an excited QD serves as a donor to transfer this excitation through non-radiative dipole-dipole interactions to neighbouring QD serving as an acceptor. While the re-absorption effect becomes significant especially in cases of high optical density samples,

^a Institute of Chemistry and the Center for Nanoscience and Nanotechnology, the Hebrew University of Jerusalem, Jerusalem, 91904, Israel.

Electronic Supplementary Information (ESI) available. See DOI: 10.1039/x0xx00000x

the FRET interaction takes place in instances in which particles are in close proximity as is often required in thin fluorescent layers.

These effects present a limitation for the use of QDs in printing applications, in which maintaining high efficiency of the fluorescence along with the control of its optical properties are crucial. This issue is of high relevance while using spherical QDs, for example in displays.

Here, we present a new and efficient solution to this problem by printing inks containing seeded semiconductor nanorods (NRs) as the fluorescent active colorant.⁴⁰⁻⁴⁴ These NRs were previously reported as applicable for lasing and light emitting diode devices and were demonstrated as more efficient than the spherical QDs for various applications such as sensitizers in solar cells and absorbers in neuronal-stimulation.⁴⁵⁻⁵¹ For these NRs the spectral overlap of the absorption and the emission spectra is reduced significantly due to the large volume of the rod compared to the emitting seed. Furthermore, the special seeded rods geometry inherently reduces significantly the detrimental effects of FRET interactions with neighbouring NRs. As will be discussed below, the use of fluorescent NRs for inkjet printing application is therefore offering significant advantages over the spherical QDs.

Here we demonstrate the inkjet printing of seeded NRs inks. For this purpose, CdSe/CdS seeded NRs are used as tuneable pigments, covering green to red emitting inks. These NRs are adjusted for dispersion in organic based solutions, while proven suitable for printing on a variety of substrates. We reveal the advantages of using seeded NRs for inkjet printing by conducting a thorough comparison of the optical properties of the NRs and QDs in this context. Both steady state and time-resolved fluorescence measurements were performed to investigate these effects. This reveals an improved performance in printing of fluorescent seeded nanorods that is of relevance for a variety of applications.

Results and discussion

Inkjet printing of fluorescent NRs inks

Emitting CdSe seeded CdS NRs (CdSe/CdS NRs) as the fluorescent pigment were dispersed in solvents to form the ink formulations. The CdSe/CdS NRs used as fluorescent pigments were prepared using a previously reported method.⁴¹ Briefly, in a first stage, synthesis of CdSe seeds was conducted by the reaction of cadmium and selenium precursors, and in the second stage the seeds were injected along with sulphur to a hot flask containing cadmium Oxide and stabilizing ligands, thus enabling the growth of the CdS rod. For more details on the synthesis see the experimental section below. Figure 1a shows a TEM image of green emitting seeded NRs (31x4.2nm) used herein. The emission colour of the NRs is tuned across the visible range by changing in particular the dimensions of the seed NCs, and further tuning the diameter of the rods. The

CdSe/CdS seeded NRs are highly emissive with a QY ranging from 40 to 90%, while dispersed in toluene.

For the solvent based ink formulations we used the NRs with alkyl-phosphonic acid and alkyl-phosphine ligands attached to the NCs surface during the synthesis stage. The NRs were dispersed in 90% dipropylene glycol methyl ether acetate (DPMA) and 10% propylene glycol methyl ether acetate (PMA) while using a dispersion agent, as described in the experimental section. In order to achieve high quality printing various properties of the formulation were adjusted such as the viscosity, evaporation rate, substrates wetting, and surface tension. Typical parameters of the inks were as follows: Viscosity of 2.0 cPs and surface tension of 28.4 dyne /cm. Proper evaporation was achieved by using two solvents with high and low evaporation rates using a 1:9 mixture ratio as described in the experimental section. The high quality of dispersion of the NRs and the maintenance of their high QY are both important aspects for the integration of the NRs within ink formulations. The particle size distribution of the NRs in the ink formulation was characterized using dynamic light scattering (DLS) analysis, as can be seen in Figure 1b. Repeatable DLS measurements for these results are presented in Figure S1 in the supporting information on-line. While the DLS method analysis is tailored for spherical particle model, it still provides a qualitative measure for comparative analysis, even for the NRs. With this in mind, it is observed that the average size (Figure 1b) of the green emitting NRs in the ink formulation with a value of 21nm (black curve) correlates to the average size of the NRs in toluene with a value of 25nm (red curve), which indicates the high quality dispersion of the NRs in the ink formulation. These results also show a similarity to the average NRs length obtained by TEM analysis, with a value of 31nm. A small fraction of the particles is seen at large sizes, but this is similar for the NRs dispersed in both the toluene and in the inks formulation. Figure 1b top inset shows the TEM image of the green emitting nanorods dispersed within the ink formulation. As clearly seen in the image, the NRs do not show aggregation or a structure modification upon their integration in the ink. Figure 1b inset bottom shows a TEM image of the ink formulation with (left) and without (right) TEM exposure. The dispersion of NRs in the ink formulation was found to be stable with no changes in particles sizes for more than 45 days at ambient conditions. Patterns of the fluorescent inks were printed by an Omnijet 100 inkjet printer. Figure 1c shows a printed signage of fluorescent NRs inks in two colours, green (31/4.2nm) and red (25/5.2nm), printed on Perspex. The printed pattern was illuminated by blue light emitting diodes (LEDs at 455nm). The emission from the printed fluorescent pattern is clearly observed. The same signage under ambient light appears nearly transparent (Figure S2). We further confirmed that the NRs inks are suitable for inkjet printing on a variety of substrates including glass, teslin paper, polycarbonate, and silicon, and that the ink formulations show dispersion and optical stability over time.

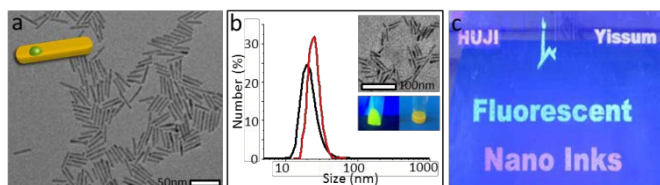


Fig. 1 a) TEM image of seeded NRs used as colour pigment for the ink formulation. Inset shows a cartoon of the seeded NRs architecture. b) Dynamic light scattering measurements of the green emitting seeded NRs in toluene (red) and in ink formulation (black). Top inset: TEM image of the green emitting seeded nanorods dispersed in ink formulation. Bottom inset: the green emitting seeded nanorods ink formulation under UV light (left) and visible light (right). c) Green (31/4.2nm) and red (25/5.2nm) emitting CdSe/CdS seeded NRs printed on thick Perspex exposed to blue LED illumination.

Optical properties of printed nanorods versus printed quantum dots

Following the successful preparation of NRs ink formulations, and demonstrating successful printing which exhibit intense fluorescence from the printed patterns, we next focused on characterizing the unique optical characteristics of the NRs inks, in comparison with QDs inks formulations. The core/shell QDs used for the comparative inks were prepared by the successive ion layer adsorption and reaction (SILAR) method.^{52, 53} During this procedure, a layer by layer growth of the CdS shell is conducted by the alternating injection of cadmium and sulphur precursors to the CdSe cores (as described fully in the experimental section).

The NRs inks show excellent stability of the fluorescence properties upon multi-layer printing. We quantitatively studied the advantages of replacing the commonly reported QDs with the NRs inks. Energy transfer and self-absorption phenomena should be more strongly pronounced in QDs structures in comparison with NRs, due to differences in the overlap between the absorption and emission spectra. Figure 2a shows the absorption (black line) and emission (green line) spectra of CdSe/CdS seeded NRs used as the pigment of the green light emitting NRs ink. As can be seen, the overlap between the emission and the absorption is insignificant, due to the relatively large volume of the CdS rod in comparison with the volume of the CdSe seed, which serves as the emission center of the NC. Figure 2b shows also the absorption (dashed black) and emission (dashed blue) of green light emitting CdSe/CdS QDs ink. For the QDs, the overlap between the emission and absorption spectra is significantly larger due to the relatively similar volume of the CdS shell and the CdSe core.

We further examined the effect of the nanocrystal structure on the optical properties of the printed arrays by testing printed samples containing NRs and QDs at different quantities. In order to achieve an accurate comparison between the different NCs, the same surface chemistry and ink formulations were used for both structures, as described in the experimental section. Since the QDs were dispersed in the same ink formulation used for the printing of the NRs inks, the

differences in the optical behaviour between the NRs and QDs inks are caused solely by the differences in their architecture.

Figure 2c shows the emission intensity at the peak wavelength with excitation at 450nm of NRs (green) and QDs (blue) printed on glass at various optical densities (O.D). We have found that there is a linear correlation between the number of layers and the calculated optical density of the printed sample (Figure S3). The best way to express this behaviour is by using the optical densities data, at the excitation wavelength of 450nm, for the comparisons presented herein. The emission of the printed QDs first shows a slight increase of the intensity caused by increase in emitter concentration on the substrate obtained by printing increasing numbers of layers, which is then followed by saturation and then even a decrease in the emission intensity already at a relatively low optical density value of 0.14. In contrast, the intensity of the printed NRs increases linearly with the increased number of printed layers without showing saturation nor quenching of intensity with thickness. This provides a direct method to achieve increasing fluorescence intensity from thicker rods layer, which is possible while using QDs.

This clear advantage of the NRs inks is further emphasized in Figure 2d which shows the measured external fluorescence quantum yield (QY) of the same printed arrays of NRs (green) and QDs (blue). As the quantity of the printed material increases, the QY of the printed NRs remains remarkably stable, while the QY of the spherical dots decreases dramatically already at very low optical density values.

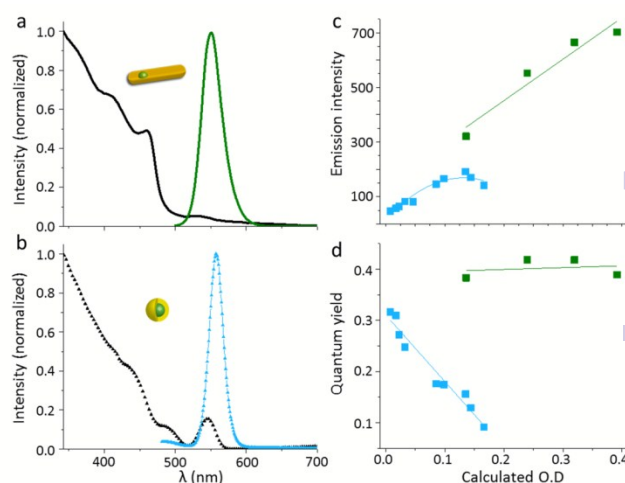


Fig. 2 a) absorption (black) and emission (green) spectra of CdSe/CdS seeded NRs used for green light emitting ink. b) Absorption (dashed black) and emission (dashed blue) spectra of CdSe/CdS core/shell QDs used for ink formulation. c) Emission intensity of green emitting seeded NRs with dimensions of 31/4.2nm (green) and green emitting QDs with diameter of 3.1nm (blue) printed arrays at different optical densities at 450nm. All samples were excited at 450nm. Calculated optical densities were determined analytically using the Hamamatsu instrument. d) Quantum yield values of the same printed NRs (green) and QDs (blue) measured using absolute QY measurement system and excited at 450nm.

The differences in the optical behaviour between the printed NRs inks and QDs inks are also notable by examining the emission spectra of the printed arrays. Figure 3a shows the emission spectra of printed NRs and QDs at various optical densities (visualization of the emission of the printed NR patterns under UV light is shown in the inset). The emission curves of the printed NRs with low O.D value (light green) and high O.D value (dark green) remain similar upon the printing of more layers of ink, while a notable emission shift to longer wavelength is seen between the printed QDs with low thickness value (light blue) to the high thickness value (dark blue). Figure 3b shows the emission wavelength shift of printed arrays of NRs and QDs measured at various values of optical densities. While the emission shift of the printed NRs is minor and within the error of the instrument, the printed QDs show a significant shift of the emission peak with the increase in ink layers by up to a value of 8nm, even for this QD sample which has a very narrow emission bandwidth. The negligible shift in the emission of the NRs enables the printing of multiple-layer arrays without the concern of change of the emission colour. This is important for the application of inkjet printing in which multiple-layers are needed for achieving high quality print. Similar optical behaviour of stable emission wavelength and QY is seen also for the red emitting NRs inkjet printed layers (Figure S4).

We also observed that the significant decrease in the QYs and the shift in the emission wavelength for the printed QDs occur at a much lower optical densities than for the solution dispersions of the same type of particles (Figure S5). This indicates that the close packing of particles in the printed arrays enhances the particle-particle interactions on the substrate compared to the liquid state, where there are large interparticle distances. For the NCs printed on substrate, dipole-dipole interactions also induce FRET interactions between the close distanced particles. Therefore, energy transfer occurs in addition to the self-absorption effect, which is the main effect for the liquid dispersions or for sparsely spaced QDs at high optical density. This interplay of mechanisms for the optical behaviour is also supported by lifetime measurements for the printed patterns and for the liquid formulations. Figure 3c shows the lifetime decay curves of printed NRs with optical density values of 0.14 (light green) and 0.41 (dark green) in comparison with printed QDs at optical density values of 0.017 (light blue), and 0.17 (dark blue) that correlate to the data presented in figure 3a. As clearly seen, the QDs show a significant shortening in the lifetime upon the addition of printed material, while the printed NRs exhibit negligible change in the lifetime decay in multi-layers. Furthermore, Figure 3c inset shows the lifetime curves of QDs inks solutions at optical density values of 0.032 (light blue) and 1.64 (dark blue). In contrast to the behaviour of the printed arrays, the dispersions show an elongation of the lifetime upon the increase in the optical density. This kind of elongation of

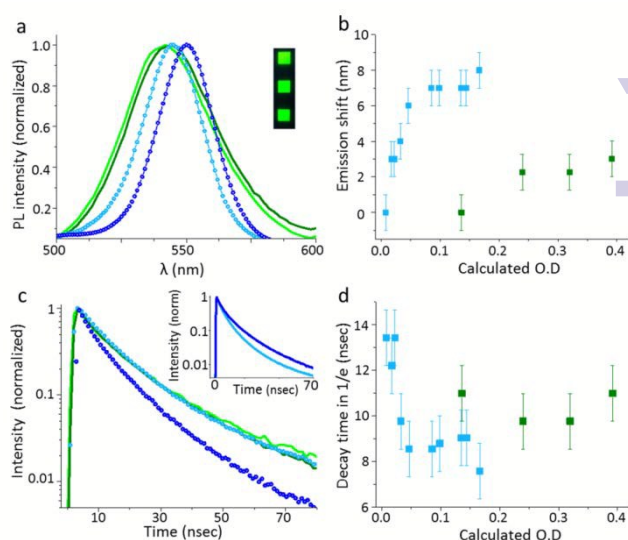


Fig. 3 a) Emission spectra of printed NRs with O.D = 0.14 (light green), and O.D = 0.41 (dark green) versus printed QDs with O.D = 0.017 (light blue), and O.D = 0.17 (dark blue). All O.D values are at the excitation wavelength of 450nm. Inset: printed squares of green emitting NRs at different optical densities under UV light. The printed arrays show no significant difference in the emission colour with increased number of layers of printed material. b) Emission shift of printed NRs and QDs at different optical densities. For the printed NRs the emission wavelength remain stable with the increase in number of layers of printed material, while there is a significant wavelength red shift for the printed QDs at higher optical densities. c) Lifetime measurements of printed NRs with O.D = 0.14 (light green) and O.D = 0.41 (dark green) versus printed QDs with O.D = 0.017 (light blue), and O.D = 0.17 (dark blue). Inset: lifetime measurements of QDs ink solutions with O.D = 0.032 (light blue), and O.D = 1.64 (dark blue). As the optical density of the QD ink increases, the lifetime is elongated, which indicates the self-absorption effect within the QD solutions. d) Effective lifetime values taken at the emission intensity reaching 1/e for printed NRs and QDs at different optical densities. Upon the increase in number of layers of printed material, the effective lifetime of the NRs remains constant, while for the QDs a shortening in the lifetimes is observed, which indicates the occurrence of a FRET process between the proximal spherical nanoparticles on the substrate.

lifetimes is typical for a self-absorption phenomenon.^{54, 55} These effects are quantified in Figure 3d, which shows the effective lifetime taken at intensity value of 1/e for the printed NRs and QDs at various optical densities. The effective lifetime of the QDs shows a systematic decrease upon the addition of layers, by a factor of nearly 2 between the low O.D and the high O.D samples. In contrast, the lifetime of the NRs remains constant within the error value of the measurements. The reduction in the QD emission lifetime is attributed to the FRET interaction between the printed particles. However, due to the unique architecture of the seeded NRs, for which the CdS emission centers are separated from one another by the large CdS rod regions, the inherent FRET interactions are significantly reduced and hence no energy transfer is seen. We further established the relevance of FRET interactions between the printed QDs by varying the percentage of dispersant molecules within the ink formulation. The addition of dispersants increases the distance between the QDs printed on the substrate and hence is expected to reduce the FRET, a process that is highly dependent on the donor-acceptor proximity on the 5-10nm length scale. Ink formulation with 4

%wt of dispersant was compared to the 1 %wt dispersant in the original QDs inks. Figure 4 shows the QY values, emission intensities, and effective lifetimes (Figures 4a, 4b, and 4c respectively) of 4.5% dispersant QDs (red) and 1% dispersant QDs (blue), together with the results for printed NRs (green) that are shown again for comparison. As clearly seen, upon increasing the amount of printed material, at high dispersant concentration the QY values are similar, an increase in the emission intensity is observed, and the lifetime decays remain similar for the samples containing higher percentage of dispersant. These optical features clearly imply that FRET interactions are more pronounced between the printed QDs in the original ink formulation containing 1 %wt of dispersant molecules. These experimental results are also supported in the literature, for which the emission properties of printed QDs were improved by the addition of polymers.²⁹ The cartoon presented in Figure 4d demonstrates the NCs arrangement within the printed arrays of NRs, QDs with 1 %wt dispersant, and QDs with 4.5 %wt dispersant (top to bottom respectively).

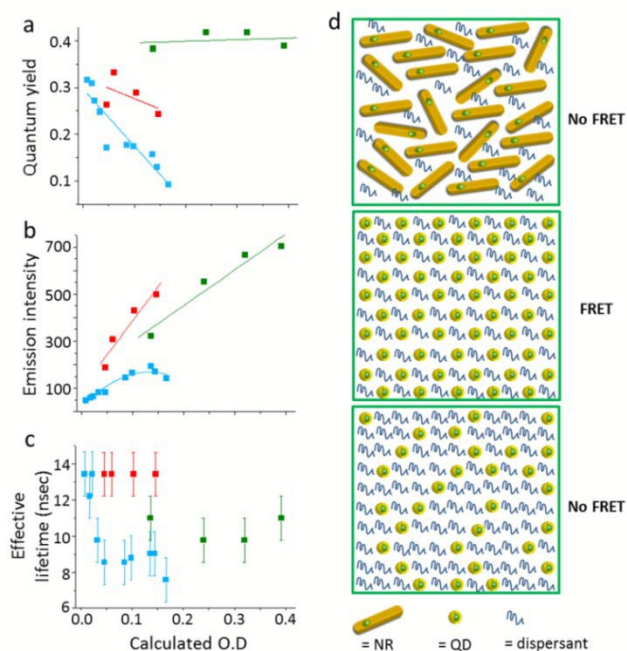


Fig. 4 a) Quantum yield of printed QDs containing 1 %wt (blue) and 4.5 %wt (red) of dispersant molecules. b) Emission intensity of the same samples of ink with 1 %wt (blue) and 4.5 %wt (red) of dispersant. c) Effective lifetime taken at the decay at $1/e$ of printed ink with 1 %wt (blue) dispersant in comparison with 4.5 %wt (red) dispersant. As the number of the dispersant molecules increases, the distance between the particles elongates and the FRET process is less pronounced. The QY remains stable for the samples containing a higher percentage of dispersant, and a significant increase in the emission intensity is also observed for these samples, with increased thickness. The lifetime curves of the printed arrays containing higher quantity of dispersant show no significant change with the addition of printed material, which indicates that no significant FRET is occurring between the nanoparticles, due to the relatively longer distance caused by the addition of dispersant molecules. Results for printed NRs (green) in 4a-c are shown again for comparison. d) A cartoon demonstrating the printed arrays of NRs, QDs with 1 %wt dispersant, and QDs with 4.5 %wt dispersant (top to bottom). For the NRs and for the QDs with higher percentage of dispersant, no FRET is observed due to relatively large distance between the emission centers of the nanoparticles, while for the printed samples containing QDs with 1 %wt of dispersant a significant FRET effect is present due to the close proximity of the QDs.

For both NRs and for QDs with a higher percentage of dispersant, lower FRET interactions occur between the printed NCs, due to the relatively larger distance between the emission centers of the NCs. Clearly though, while the QDs ink require a special treatment such as the addition of further dispersant or polymer in order to achieve an improvement in their photoluminescence performance, the properties of the unique NRs inks remain constant in multi-layer inkjet printing without further chemical manipulations.

Experimental section

Materials

Trioctylphosphine oxide (TOPO), trioctylphosphine (TOP), octadecylphosphonic acid (ODPA), hexylphosphonic acid (HPA), cadmium oxide, selenium powder 99%, sulfur powder 99%, octadecylamine (ODA), octadecene (ODE), dipropylene glycol methyl ether acetate (DPMA), and propylene glycol methyl ether acetate (PMA), were purchased from Sigma Aldrich. The surface active material Surfonomine L-100, was received from Huntsman, Netherlands.

Synthesis of seeded NRs

The synthesis was performed as follows: (All procedures carried out using inert atmosphere in Schlenk line). The CdSe cores were synthesized based on reported procedures with modifications.⁴¹ In a typical procedure for synthesis of CdSe cores, a reaction flask containing cadmium oxide (0.018 g), TOPO (3 g), ODPA (0.56 g), and TOP (1.8 mL) was placed under vacuum at 100 °C for half an hour. The solution was then heated to 350 °C under argon, followed by the fast injection of selenium powder (0.014 g) in TOP solution (72 μL). At this point, the colour of the solution changes from colourless to yellow, which indicates the formation of CdSe QDs. The size of the nanocrystals is controlled by the CdSe time growth. For the green and yellow emitting NRs the diameter of the cores is between 2.2nm to 2.4nm, while for the red emitting NRs the diameter of the cores is between 3.0nm to 3.4nm. CdSe/CdS seeded nanorods were synthesized using modified procedure.⁴¹ In a typical NRs synthesis, a solution containing previously prepared CdSe cores (8×10^{-6} mole) in TOP (1.8 mL) is premixed with sulphur powder (0.02 g). For the green emitting seeded NRs, cores with 2.2nm diameter were used. For the red emitting seeded NRs CdSe cores with a diameter of 3.3nm were used. For the seeded rods growth, The core solution was injected to a reaction flask containing cadmium Oxide (0.08 g), TOPO (3 g), ODPA (0.29 g), and HPA (0.08 g) that was previously degassed under vacuum at 100 °C for half an hour. The injection temperature was set to 360 °C under argon. The synthesis lasted for 8 minutes, in which the growth of the CdS rod took place.

Synthesis of CdSe/CdS core/shell QDs

The QDs were synthesized by the successive ion layer adsorption and reaction (SILAR) method.⁵² In this core/shell QDs synthesis, a sequential layer by layer growth of cadmium and Sulphur is applied on the CdSe cores. The quantities of the precursors needed for

growth of a CdS mono-layer were pre-calculated in advance and modified for different diameter of the CdSe cores. The cadmium and Sulphur both in ODE were slowly injected to a solution containing CdSe cores (1.5×10^{-7} mole) in ODE (5 mL) and ODA (3 g). The temperature was then raised to 120 °C under vacuum, and stirred for half an hour. The injection of the cadmium precursor for the first cadmium layer was performed at 190 °C. The first Sulphur portion was injected 30 minutes later under the same conditions. After each monolayer the temperature was raised by 10 °C degrees until the reaction temperature was set on 240 °C. The time between each injection was set to half an hour, in which the layer growth and annealing is occurring. For the preparation of the green emitting QDs described in this manuscript, a CdSe cores with diameter of 2.5nm were used for the growth of three monolayers of CdS shell. The overall diameter of the core/shell structure is 3.1nm.

Surface ligand exchange on the QDs

Ligand exchange from ODA to the alkyl-phosphonic acid and alkyl-phosphine ligands was conducted by adding TOPO (3 g), ODPA (0.56 g), and TOP (1.8 mL) to previously cleaned QDs dispersed in toluene solution (2 mL). The QDs were then mixed and refluxed at 100 °C for two hours.

Ink formulation preparation

The ink formulations were prepared as follow: The NCs were first cleaned and washed from excess of ligands and precursors by precipitation with methanol, followed by centrifugation and drying. Then, the NCs powder (0.04 g) was added to solvents mixture containing 90% DPMA and 10% PMA (2.92 g). Huntsman surfonamine (R) L-100 (0.04 g) was then added as the dispersing agent for the NCs. In order to obtain the optimal dispersibility of the NCs within the ink formulation, various concentrations of NCs and dispersant were evaluated in preliminary experiments. Bath sonication and horn sonication were applied for 30 min each along with stirring on vortex for a few minutes, in order to improve the dispersion of the NCs within the ink formulation.

The printing procedure

The printing was carried out using an Omnijet 100 (Unijet, Korea) printer equipped with Diamtix 30 picoliters piezoelectric printing head. The temperature of the substrate was set to 80 °C. Ink (1 mL) was loaded to the cartridge and used for printing experiments at 2500 Hz, with waveform characteristics of 2 µsec rise and fall times, and 5 µsec at 40 volts. For the optical analyses, square patterns (1cm by 1cm) were printed, composed of 250 rows and columns with 50 microns spaces between the lines.

Quantum yield measurements

The QY values obtained for both solutions and printed patterns were measured directly using the Hamamatsu absolute photoluminescence QY Spectrometer C11347 Quantaaurus - QY. The instrument measures the absorption and the emission of the sample within an integrated sphere and extracts its QY value.

Correction of the QY by neglecting self-absorption in solutions is another feature of the instrument and is used for the determination of the most accurate QY of the solutions, without re-absorption effects. The QY values extracted by this method are absolute and therefore are more reliable than the data extracted by the commonly applied relative method, which uses an organic dye with a known QY as a reference. Both the nanoparticles solutions and the nanoparticles printed films are measured using this technique using a special sample container.

Fluorescence lifetime measurements

The lifetime measurements were carried out using a fluorescence spectrometer (Edinburgh Instruments FLS920) equipped with a film holder. The samples were excited at 405nm, 0.2 MHz rate, using picosecond pulsed diode laser EPL-405. The fluorescence lifetime were measured at 550nm \pm 5nm using a high speed photomultiplier and time-correlated single photon counting.

Conclusions

We presented an efficient approach for inkjet printing of fluorescent NCs. Printing of seeded NRs allows to maintain the optical properties including the emission colour, its QY and its stability. While previous printing of QDs suffer from changes in fluorescence properties upon changing the thickness of the printed material, the printed NRs maintains both the high QY and the emission peak wavelength without shifts. Here we presented the functionality of these unique fluorescent NRs in organic based inkjet ink formulations, but the results and conclusions are of relevance also for other printing technologies that can be applied, upon proper tailoring of the ink formulation. We showed here the particle morphology effect for cadmium chalcogenide materials, which are outstanding model systems in terms of their highly developed synthesis control and understanding of properties, as proof of concept. The findings are relevant also for future generations of nanocrystals without Cd, with similar geometries. The NRs based inks show significant potential for use in a variety of applications including signage, displays, security inks and optoelectronic devices.

Acknowledgements

This work was financially supported by the Israel National Nanotechnology Initiative, under the focal technologies areas program (FTAs). UB thanks the Alfred and Erica Larsson Memorial Chair.

Notes and references

- 1 A. Sitt, I. Hadar and U. Banin, *Nano Today*, 2013, **8**, 494.
- 2 D. V. Talapin, J. S Lee, M. V. Kovalenko and E. V. Shevchenko, *Chem. Rev.*, 2009, **110**, 389.
- 3 M. V. Kovalenko, L. Manna, A. Cabot, Z. Hens, D. V. Talapin, C.R. Kagan, V. I. Klimov, A. L. Rogach, P. Reiss, D. J. Milliron,

- P. G Sionnest, G. Konstantatos, W. J. Parak, T. Hyeon, B. A. Korgel, C. B. Murray and W. Heiss, *ACS Nano*, 2015, **9**, 1012.
- 4 P. Reiss, M. Protière and L. Li, *Small*, 2009, **5**, 154.
 - 5 W. J. Stark, *Angew. Chem. Int. Ed.*, 2011, **50**, 1242.
 - 6 W. J. Parak, D. Gerion, T. Pellegrino, D. Zanchet, C. Micheel, S. C. Williams, R. Boudreau, M. A Le Gros, C. A. Larabell and A. P. Alivisatos, *Nanotechnology*, 2003, **14**, R15.
 - 7 L. Xu, L. Wang, X. Huang, J. Zhu, H. Chen, and K. Chen, *Physica E*, 2000, **8**, 129.
 - 8 R. A. Sperling and W. J. Parak, *Phil. Trans. R. Soc. A*, 2010, **368**, 1333.
 - 9 S. Wilhelm, M. Kaiser, C. Würth, J. Heiland, C. Carrillo-Carrion, V. Muhr, O. S. Wolfbeis, W. J. Parak, U. Resch-Genger and T. Hirsch, *Nanoscale*, 2015, **7**, 1403.
 - 10 D. Dorokhin, S. H. Hsu, N. Tomczak, D. N. Reinhoudt, J. Huskens, A. H. Velders and G. J. Vancso, *ACS Nano*, 2010, **4**, 137.
 - 11 A. C. Arango, D. C. Oertel, Y. Xu, M. G. Bawendi and V. Bulović, *Nano Lett.*, 2009, **9**, 860.
 - 12 M. J. Panzer, K. E. Aidala, P. O. Anikeeva, J. E. Halpert, M. G. Bawendi and V. Bulović, *Nano Lett.*, 2010, **10**, 2421.
 - 13 D. Zhou, A. Bruckbauer, C. Abell, D. Klenerman and D. J. Kang, *Adv. Mater.*, 2005, **17**, 1243.
 - 14 S. J. P. Kress, P. Richner, S. V. Jayanti, P. Galliker, D. K. Kim, D. Poulikakos and D. J. Norris, *Nano Lett.*, 2014, **14**, 5827.
 - 15 T. H. Kim, K. S. Cho, E. K. Lee, S. J. Lee, J. Chae, J. W. Kim, D. H. Kim, J. Y. Kwon, G. Amaratunga, S. Y. Lee, B. L. Choi, Y. Kuk, J. M. Kim and K. Kim, *Nat. Photonics*, 2011, **5**, 176.
 - 16 S. Kim, S. H. Im and S. W. Kim, *Nanoscale*, 2013, **5**, 5205.
 - 17 L. A. Kim, P. O. Anikeeva, S. A. Coe-Sullivan, J. S. Steckel, M. G. Bawendi and V. Bulović, *Nano Lett.*, 2008, **8**, 4513.
 - 18 P. O. Anikeeva, J. E. Halpert, M. G. Bawendi and V. Bulovic, *Nano Lett.*, 2009, **9**, 2532.
 - 19 A. Rizzo, M. Mazzeo, M. Biasiucci, R. Cingolani and G. Gigli, *Small*, 2008, **4**, 2143.
 - 20 A. Rizzo, M. Mazzeo, M. Palumbo, G. Lerario, S. D'Amone, R. Cingolani and G. Gigli, *Adv. Mater.*, 2008, **20**, 1886.
 - 21 E. Jang, S. Jun, H. Jang, J. Lim, B. Kim and Y. Kim, *Adv. Mater.*, 2010, **22**, 3076.
 - 22 S. Magdassi, *The Chemistry of Inkjet Inks*, World Scientific Publishing Co. Pte. Ltd: Singapore, 2009.
 - 23 M. Grouchko, A. Kamysny and S. Magdassi, *J. Mater. Chem.*, 2009, **19**, 3057.
 - 24 A. Kamysny, M. Ben-Moshe, S. Aviezer and S. Magdassi, *Macromol. Rapid Comm.*, 2005, **26**, 281.
 - 25 B. K. Park, D. Kim, S. Jeong, J. Moon and J. S. Kim, *Thin Solid Films*, 2007, **515**, 7706.
 - 26 J. Niittynen, E. Sowade, H. Kang, R. R. Baumann and M. Mäntysalo, *Scientific Reports*, 2015, **5**, 8832.
 - 27 Z. Zhang, X. Zhang, Z. Xin, M. Deng, Y. Wen and Y. Song, *Adv. Mater.*, 2013, **25**, 6714.
 - 28 B. Bao, M. Li, Yuan Li, J. Jiang, Z. Gu, X. Zhang, L. Jiang and Y. Song, *Small*, 2015, **11**, 1649.
 - 29 E. Tekin, P. J. Smith, S. Hoepfner, A. M. J. van den Berg, A. S. Susha, A. L. Rogach, J. Feldmann and U. S. Schubert, *Adv. Funct. Mater.*, 2007, **17**, 23.
 - 30 V. Wood, M. J. Panzer, J. Chen, M. S. Bradley, J. E. Halpert, M. G. Bawendi and V. Bulović, *Adv. Mater.*, 2009, **21**, 2151.
 - 31 H. M. Haverinen, R. A. Myllylä and G. E. Jabbour, *Appl. Phys. Lett.*, 2009, **94**, 073108.
 - 32 H. M. Haverinen, R. A. Myllylä and G. E. Jabbour, *J. Disp. Technol.*, 2010, **6**, 87.
 - 33 J. Y. Kim, C. Ingrosso, V. Fakhfour, M. Striccoli, A. Agostiano, M. L. Curri and J. Brugger, *Small*, 2009, **5**, 1051.
 - 34 A. M. Elliott, O. S. Ivanova, C. B. Williams and T. A. Campbell, *Adv. Eng. Mater.*, 2013, **15**, 903.
 - 35 E. Binetti, C. Ingrosso, M. Striccoli, P. Cosma, A. Agostiano, K. Pataky, J. Brugger and M. L. Curri, *Nanotechnology*, 2012, **23**, 075701.
 - 36 C. Ingrosso, J. Y. Kim, E. Binetti, V. Fakhfour, M. Striccoli, A. Agostiano, M. L. Curri and J. Brugger, *Microelectron. Eng* 2009, **86**, 1124.
 - 37 N. Marjanovic, J. Hammerschmidt, J. Perelaer, S. Farnsworth, I. Rawson, M. Kus, E. Yenel, S. Tilki, U. S. Schubert and R. P. Baumann, *J. Mater. Chem.*, 2011, **21**, 13634.
 - 38 A. C. Small, J. H. Johnston and N. Clark, *Eur. J. Inorg. Chem* 2010, **242**.
 - 39 J. R. Lakowicz, *Principles of Fluorescence Spectroscopy Third ed*, Springer Science+Business Media, LLC, New York 2006.
 - 40 D. V. Talapin, R. Koeppel, S. Gotzinger, A. Kornowski, J. M. Lupton, A. L. Rogach, O. Benson, J. Feldmann and H. Welle, *Nano Lett.*, 2003, **3**, 1677.
 - 41 L. Carbone, C. Nobile, M. De Giorgi, F. D. Sala, G. Morello, P. Pompa, M. Hytch, E. Snoeck, A. Fiore, I. R. Franchini, M. Nadasan, A. F. Silvestre, L. Chiodo, S. Kudera, R. Cingolani, P. Krahne and L. Manna, *Nano Lett.*, 2007, **7**, 2942.
 - 42 A. Sitt, A. Salant, G. Menagen and U. Banin, *Nano Lett.*, 2011, **11**, 2054.
 - 43 D. Dorfs, A. Salant, I. Popov and U. Banin, *Small*, 2008, **4**, 1319.
 - 44 D. V. Talapin, J. H. Nelson, E. V. Shevchenko, S. Aloni, M. Sadtler and A. P. Alivisatos, *Nano Lett.*, 2007, **7**, 2951.
 - 45 H. Pühringer, J. Roither, M. V. Kovalenko, M. Eibelhuber, T. Schwarzl, D. V. Talapin and W. Heiss, *Appl. Phys. Lett.*, 2010, **97**, 111115.
 - 46 M. Zavelani-Rossi, M. G. Lupo, R. Krahne, L. Manna and G. Lanzani, *Nanoscale*, 2010, **2**, 931.
 - 47 A. Rizzo, C. Nobile, M. Mazzeo, M. De Giorgi, A. Fiore, L. Carbone, R. Cingolani, L. Manna and G. Gigli, *ACS Nano*, 2009, **3**, 1506.
 - 48 A. Salant, M. Shalom, Z. Tachan, S. Buhbut, A. Zaban and U. Banin, *Nano Lett.*, 2012, **12**, 2095.
 - 49 L. Bareket, N. Waiskopf, D. Rand, G. Lubin, M. David-Pur, M. Ben-Dov, S. Roy, C. Eleftheriou, E. Sernagor, O. Cheshnovsky, U. Banin and Y. Hanein, *Nano Lett.*, 2014, **14**, 6685.
 - 50 M. Zanella, R. Gomes, M. Povia, C. Giannini, Y. Zhang, A. Riskin, M. Van Bael, Z. Hens and L. Manna, *Adv. Mater* 2011, **23**, 2205.
 - 51 A. Persano, M. De Giorgi, A. Fiore, R. Cingolani, L. Manna, A. Cola and R. Krahne, *ACS Nano*, 2010, **4**, 1646.
 - 52 J. J. Li, Y. A. Wang, W. Guo, J. C. Keay, T. D. Mishima, M. Johnson and X. Peng, *JACS*, 2003, **125**, 12567.
 - 53 R. Xie, U. Kolb, J. Li, T. Basche and A. Mews, *JACS*, 2004, **127**, 7480.
 - 54 M. Y. Berezin and S. Achilefu, *Chem. Rev.*, 2010, **110**, 2641.
 - 55 J. Demas, *Excited State Lifetime Measurements*, Academic Press, INC, LTD., London 1983.